Preprint Title	Effect of induced ripples on the electronic properties of graphene monolayer: Simulation study
Authors	Mohammad S. Ahmad and Jamal A. Talla
Publication Date	27 Sep 2021
Article Type	Full Research Paper
ORCID® iDs	Mohammad S. Ahmad - https://orcid.org/0000-0002-7347-9150; Jamal A. Talla - https://orcid.org/0000-0003-4877-2870

Effect of induced ripples on the electronic properties of graphene monolayer: Simulation study

Mohammad S. Ahmad[1] and Jamal A. Talla[1*]
[1] Department of Physics, Al al-Bayt University, Al-Mafraq - 130040, Jordan

Abstract

The effect of tensile stress on the electronic properties of pristine graphene mono-sheet was investigated. We applied different stress factors in order to investigate the mechanical and electronic properties of graphene monolayer. As a consequence of the applied tensile stress, different patterns of ripples were created. Whereas, different rippling levels were significantly tuned the electronic properties of the graphene monolayer. For instance, the band gap of graphene monolayer dramatically increased with increasing the tensile stress factor. Moreover, the combined effect of applying tensile stress as well as bending the sheet significantly modified the band gap. However, applying more tensile stress induced a reverse behavior. We highly believe that, controlling local curvatures of graphene monolayer opens up opportunities for strain assisted tuning of local electronic structure such as band gap engineered devices.

Keywords: graphene, tensile stress, electronic properties, density functional theory.

To whom the correspondence should be addressed:
jtalla@aabu.edu.jo (Jamal A. Talla)

Fax: 009626297034

I. Introduction

Recently, carbon based nanostructures has become an important aspect of the technological revolution and the new scientific revolution in various fields [1-3]. Various structures based on carbon atoms have been produced such as graphene [4-6]. Graphene, a 2-dimensional monolayer of sp^2 hybridized carbon atoms organized in honeycomb lattice [7, 8]. Furthermore, graphene has excellent mechanical properties due to its covalent bonds formed due to sp^2 hybridization making it stronger than sp^3 hybrid carbon and carbon bonds in a diamond [8]. Therefore, it is considered as one of the strongest materials in the world [9]. Due to its unique chemical structure as well as its electronic properties, graphene has gained extraordinary properties, such as; weak optical absorptivity, highest room-temperature carrier mobility, high mechanical strength, and high thermal conductivity [6, 10, 11]. Furthermore, graphene is a valuable material because of its numerous beneficial properties, in which the electronic properties is considered as the most important property. One of the distinguishing features of graphene is their electron mobility, whereas, graphene is a semiconductor material with a zero band gap [3, 7, 12].

Different production techniques were proposed like Rodney Rouff et. al who generated graphene monolayer through rubbing graphite on silicon wafers [13]. On the other hand, Philip Kim et al created graphite sheets by writing on a surface with a "nano-pencil" [14]. Such experiment produced at least ten layers of graphene, whereas, their experiment brings the idea of generating graphene one step forward. Moreover, Andre Geim et. al

used a method to isolate graphene with the aid of a technique called micromechanical cleavage, or "the scotch tape" method [15].

2-dimensional nanomaterial's exhibits surface corrugations. Thermaledge instabilities, vibrations, and strain in 2-dimensional crystals might generate ripples on graphene monolayer [5, 16]. These surface modifications on graphene may play a crucial rule not only on tuning the electronic properties of graphene monolayer but also induce pseudomagnetic field that create polarized carrier puddles, in bilayers which in turn alter surface properties [17]. For that purpose, we aim to induce ripples on the surface of graphene monolayer by applying tensile bi-directional stress and their impact on the electronic properties of rippled graphene.

II. Computational Work

A single graphene sheet was simulated using a supercell containing 288 atoms in a two-dimensional hexagonal lattice (Figure 1). To keep the sheet periodicity, the lattice parameters of the pristine graphene mono-sheet was set as ***a=29.520*** $\overset{o}{A}$ ***, b = 29.520*** $\overset{o}{A}$ [18-20]. To prevent any interaction between the graphene mono-sheet and its image, the lattice constant ***"c"*** was set to a relatively high value ***(25*** $\overset{o}{A}$ ***).*** After that, we created 2-dimensional matrix as below:

$$\begin{pmatrix} a \backslash b & 29.52 & 28.93 & 28.34 & 27.75 & 27.16 & 26.57 \\ 29.52 & G_{11} & G_{12} & G_{13} & G_{14} & G_{15} & G_{16} \\ 28.93 & G_{21} & G_{22} & G_{23} & G_{24} & G_{25} & G_{26} \\ 28.34 & G_{31} & G_{32} & G_{33} & G_{34} & G_{35} & G_{36} \\ 27.75 & G_{41} & G_{42} & G_{43} & G_{44} & G_{45} & G_{46} \\ 27.16 & G_{51} & G_{52} & G_{53} & G_{54} & G_{55} & G_{56} \\ 26.57 & G_{61} & G_{62} & G_{63} & G_{64} & G_{65} & G_{66} \end{pmatrix} .....M(I)$$

The above matrix represents the correlation between the length and width of the graphene monolayer and the corresponding tensile stress factor, whereas; G_{ij} refer to the graphene lattice parameters after applying tensile stress factor. Upon generating ripples in the graphene monolayer, by applying bi-directional tensile stress, all calculations were performed with the aid of density functional theory using DMOL3 code implemented in density functional theory [21-24]. Before calculating all structures energy, geometry optimization was first performed with generalized gradient approximation (GGA) and revised Perdew-Burke-Ernzerhof (RPBE) parameterization [25, 26]. All 36 structures were fully optimized every time tensile stress was applied, until the force was less than 0.01 eV $Å^{-1}$. In addition, SCF tolerance, maximum displacement, and maximum stress were set as 1 x 10^{-6} eV/atom, 0.001 Å and 0.04 GPa, respectively [27, 28]. While Monkhorst-Pack grid was generated using 1 x 9 x 9 k-point, the core electrons were represented using ultra-soft pseudo-potentials [5, 16]. Finally, energy calculations with the relevant band structure calculations were performed to all geometry optimized structures.

III. Results and Discussions

The lack of band-gap energy is considered as the main obstacle limiting the use of graphene monolayer. Hence, researchers have undertaken efforts all over the globe to control the band gap in graphene.

III.I Band gap calculations

We monitored the band gap variations upon applying tensile stress, starting from a pristine graphene mono-layer. We found that the band gap of pristine graphene mono-layer was zero, such value is consistent with previous studies, refer to Figure 2(a). Upon

applying 0.94 tensile stress on the lattice parameter ***"b"*** while keeping the lattice parameter ***"a"*** fixed, the band gap significantly increased from 0.000 eV to 0.363, refer to Figure 2(c). Furthermore, increasing the stress factor to 0.90 the band gap significantly increased to 0.448 eV, refer to Figure 2(e). Moreover, the band gap linearly changes upon applying tensile stress on the graphene mono layer. This linear behavior is an excellent example for pressure sensors applications. A very special case was observed upon increasing the pressure to a certain point in both directions. In such case, the band gap returns to zero. This band gap reduction could be attributed not only to the deformation created in the graphene sheet, but also to the symmetric bond reduction. Whereas, the created ripples in the sheet is greatest when symmetric tensile stress where applied on ***"a"*** and ***"b"*** lattice parameters. It is good to mention that modifying both lattice parameters has different band gap values, more details can be found in Figure 3, 4, 5 and Table 1.

The stress converts the graphene structure from a flat structure to a rippled structure. These ripples have a significant influence on the electronic properties of graphene. It is worth mentioning that GGA approximation underestimates the band gap and the band gap opining is expected to be larger than the reported values. The change in the band gap is attributed to disorders induced by the applied stress, as these disorders lead to rotation of the p_z orbitals. When ripples are formed on the surface of the graphene, bending occurs at different amplitudes along the graphene surface depending on the applied tensile stress. Such ripples produce a rotation between p_z orbitals and as a consequence, the distance between these orbitals was reduced and in turn the p_z orbitals overlap more.

The more p_z overlapping will eventually lead to re-hybridization between π and σ orbitals refer to Figure 6 [3, 4, 29]. Furthermore, when the structure bends due to ripples, the carbons and their neighbors form a pyramid, with each carbon becoming a corner, and the flat shape of the structure is gone and the re-hybridization occurs when π orbital couples with three σ bonds Figure 6 [30-32].

To further understand the obtained results, we calculated the density of states (DOS). From the DOS we can get an insight into the gap and the differences in the occupied states. As a comparison between the DOS of the pristine graphene monolayer and the DOS graphene monolayer under different tensile stress, some discrepancies in the DOS which directly correlated to the variations in the band gap.

Moreover, in the pristine graphene monolayer, we observed that the peak intensity has one prominent peak around the Fermi level (red dashed line), refer to Figure 2(b). Upon applying tensile stress on the graphene sheet by factor stress of 0.94 towards the lattice parameter ***"b"*** with keeping the lattice parameter ***"a"*** fixed, we noticed the peak intensity has one main peak, it expanded and move slightly upwards; refer to Figure 2(d). Upon applying tensile stress on the graphene sheet by factor stress of 0.90 towards the lattice parameter ***"b"*** with keeping the lattice parameter ***"a"*** fixed, we noticed the main peak has one prominent peak with less intensity, more broadened, and shifted away from the Fermi level; refer to Figure 2 (f). Applying tensile stress on both lattice parameters has direct impact on the peaks around the Fermi level. It is good to mention that in some occasions a similar behavior were observed as not only the peak intensity had one main peak, but also it moved slightly away from the Fermi level; refer to Figures (3(d), 3(f), 4(f), 5(f)).

III.II Fermi energy valence band and conduction band

We monitored the changes in conduction band, valence band and Fermi energy for all tensile stress cases. Initially, when we applied tensile stress on the lattice parameter ***"b"*** with keeping the ***"a"*** lattice parameter fixed, we noticed that the band gap significantly increased from 0.00 eV to 0.448 eV. Such significant increase in the band gap could be ascribed to an upshift in the conduction band and down shift in the valance band, refer to Figure 7(a). Furthermore, upon applying 0.98 on the lattice parameter ***"b"*** while applying different stress factors on the lattice parameter ***"a"*** tensile stress the band gap of the graphene monolayer decreased from 0.128 eV to 0.092 eV followed by an increase in the band gap ~ 0.255 eV, refer to Figure 7(b). These variations could be explained as the valance band and conduction bands shift closely and then shift apart Figure 7.

IV. Conclusion

In this study, we used density functional theory to investigate the effect of tensile stress on the electronic properties of graphene monolayer. We found that applying tensile stress on the graphene monolayer has a direct impact on the electronic properties. We observed that applying pressure leads to different values in the band gap and the variations in the band gap values is a good example of pressure sensor applications. We also believe that our study might be useful for touch screen applications in which such valuable expectations merits further investigations. Finally, controlling the electronic properties of graphene will be useful for different electronic devices.

References

[1]J.A. Talla, Ab initio simulations of doped single-walled carbon nanotube sensors, Chemical Physics 392 (2012) 71-77.

[2]O. Stephan, P.M. Ajayan, C. Colliex, P. Redlich, J.M. Lambert, P. Bernier, P. Lefin, Doping graphitic and carbon nanotube structures with boron and nitrogen, Science 266 (1994) 1683-1685.

[3]J. Wang, F. Ma, W. Liang, M. Sun, Electrical properties and applications of graphene, hexagonal boron nitride (h-BN), and graphene/h-BN heterostructures, Materials Today Physics 2 (2017) 6-34.

[4]G. Yang, L. Li, W.B. Lee, M.C. Ng, Structure of graphene and its disorders: a review, Science and Technology of Advanced Materials 19 (2018) 613-648.

[5]J. A. Talla, E.A. Almahmoud, K. Al-Khaza'leh, H. Abu-Farsakh, Structural and electronic properties of rippled graphene with different orientations of Stone Wales defects: first-principles study, Semiconductor 55 (2021.(

[6]J.A. Talla, Pressure induced phase transition and band gap controlling in defective graphene mono-sheet: Density functional theory, Materials Research Express 6 (2019) 115012.

[7]J.A. Talla, Band Gap Opening of Doped Graphene Stone Wales Defects: Simulation Study, Semiconductors 54 (2020) 40-45.

[8]X. Huang, S. Yin Z Fau - Wu, X. Wu S Fau - Qi, Q. Qi X Fau - He, Q. He Q Fau - Zhang, Q. Zhang Q Fau - Yan, F. Yan Q Fau - Boey, H. Boey F Fau - Zhang, H. Zhang, Graphene-based materials: synthesis, characterization, properties, and applications, (2011.(

[9]V. Singh, D. Joung, L. Zhai, S. Das, S.I. Khondaker, S. Seal, Graphene based materials: Past, present and future, Progress in Materials Science 56 (2011) 1178-1271.

[10]L. Li, S. Reich, J. Robertson, Defect energies of graphite: Density-functional calculations, Physical Review B 72 (2005) 184109.

[11]E.A. Almahmoud, J.A. Talla ,H. Abu-Farsakh, Influence of uniaxial strain on the electronic properties of doped graphene mono-sheets: A theoretical study, Materials Research Express 6 (2019) 115617.

[12]E. Kaxiras, K.C. Pandey, Energetics of defects and diffusion mechanisms in graphite, Physical Review Letters 61 (1988) 2693-2696.

[13]X. Lu, M. Yu, H. Huang, R.S. Ruoff, Tailoring graphite with the goal of achieving single sheets, Nanotechnology 10 (1999) 269-272.

[14]Y. Zhang, J.P. Small, W.V. Pontius, P. Kim, Fabrication and electric-field-dependent transport measurements of mesoscopic graphite devices, Applied Physics Letters 86 (2005.(

[15]K.S. Novoselov, A.K. Geim, S.V. Morozov, D. Jiang, Y. Zhang, S.V. Dubonos, I.V. Grigorieva, A.A. Firsov, Electric field effect in atomically thin carbon films, Science 306 (2004) 666-669.
[16]J. A. Talla, E. A. Almahmoud, H. Abu-Farsakh, Rippling effect on the electrical properties of boron nitride monolayer: Density Functional theory, Semiconductor 55 (2021) 902–909.
[17]M.M. Fogler, F. Guinea, M.I. Katsnelson, Pseudomagnetic fields and ballistic transport in a suspended graphene sheet, Phys Rev Lett 101 (2008) 226804.
[18]J.A. Talla, Stability and electronic properties of hybrid coaxial carbon nanotubes–boron nitride nanotubes under the influence of electric field, Applied Physics A 127 (2021.(
[19]E.A. Almahmoud, J.A. Talla, H. Abu-Farsakh, Electronic properties of defective boron nitride mono-sheets under the influence of an external electric field, Semiconductor Science and Technology 35 (2020) 025014.
[20]J.A. Talla, A.F. Alsalieby, Effect of uniaxial tensile strength on the electrical properties of doped carbon nanotubes: Density functional theory, Chinese Journal of Physics 59 (2019) 418-425.
[21]M. Serhan, M. Abusini, E. Almahmoud, R. Omari, K. Al-Khaza'leh, H. Abu-Farsakh, A. Ghozlan, J. Talla, The electronic properties of different chiralities of defected boron nitride nanotubes: Theoretical study, Computational Condensed Matter 22 (2020) e00439.
[22]J.A. Talla, Electronic properties of silicon carbide nanotube with Stone Wales defects under uniaxial pressure: A computational study, Computational Condensed Matter 19 (2019) e00378.
[23]M. Nairata, J. Talla, Electronic Properties of Aluminum Doped Carbon Nanotubes with Stone Wales Defects: Density Functional Theory, Physics of the Solid State 61 (2019) 1896–1903.
[24]E. Almahmoud, J.A. Talla, Band gap tuning in carbon doped boron nitride mono sheet with Stone-Wales defect: a simulation study, Materials Research Express 6 (2.105038 (019
[25]J.A.S. Talla, Saed A.; Sabbah, Hussien; Yasin, Esam; Zir, Alaa Abu, Modeling Single-Walled Boron Nitride Nanotube Pressure Sensor: Density Functional Study, Nanoscience and Nanotechnology Letters 7 (2015) 500.
[26]J.A. Talla, S.A. Salman, Electronic Structure Tuning and Band Gap Engineering of Carbon Nanotubes: Density Functional Theory, Nanoscience and Nanotechnology Letters 7 (2015) 1-6.
[27]A.A. Ghozlan, J.A. Talla, OPTICAL PROPERTIES OF DEFECTIVE SILICON CARBIDE NANOTUBES: THEORETICAL STUDY, Rev. Cubana Fis. 36 (2019) 27-36.
[28]S.A. Salman, J.A. Talla, M.A. Al-Othoum, Uniaxial tension/compression effects on the electrical properties of carbon nanotube bundles: A first-principles study, Materials Express 8 (2018) 353-360.
[29]S .Deng, V. Berry, Wrinkled, rippled and crumpled graphene: an overview of formation mechanism, electronic properties, and applications, Materials Today 19 (2016) 197-212.
[30]G. Yildiz, M. Bolton-Warberg, F. Awaja, Graphene and graphene oxide for bio-sensing: General properties and the effects of graphene ripples, Acta Biomaterialia 131 (2021) 62-79.
[31]Y. Zhu, S. Murali, W. Cai, X. Li, J.W. Suk, J.R. Potts, R.S. Ruoff, Graphene and Graphene Oxide: Synthesis, Properties, and Applications, Advanced Materials 22 (2010) 3906-3924.
[32]J. Ma, D. Alfè, A. Michaelides, E. Wang, Stone-Wales defects in graphene and other planar sp^2-bonded materials, Physical Review B 80 (2009) 033407.

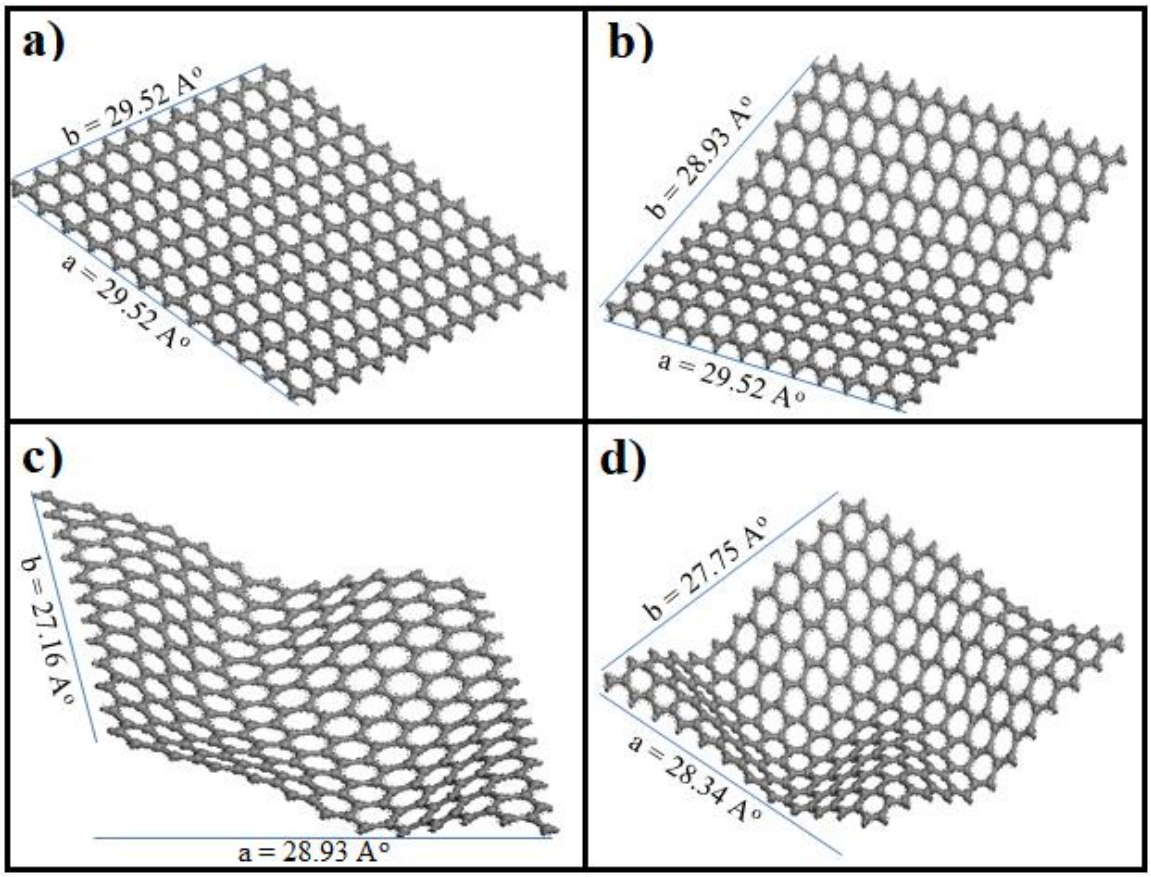

Figure 1: Pristine graphene monolayer and graphene monolayer after applying tensile stress with different selective stress factors.

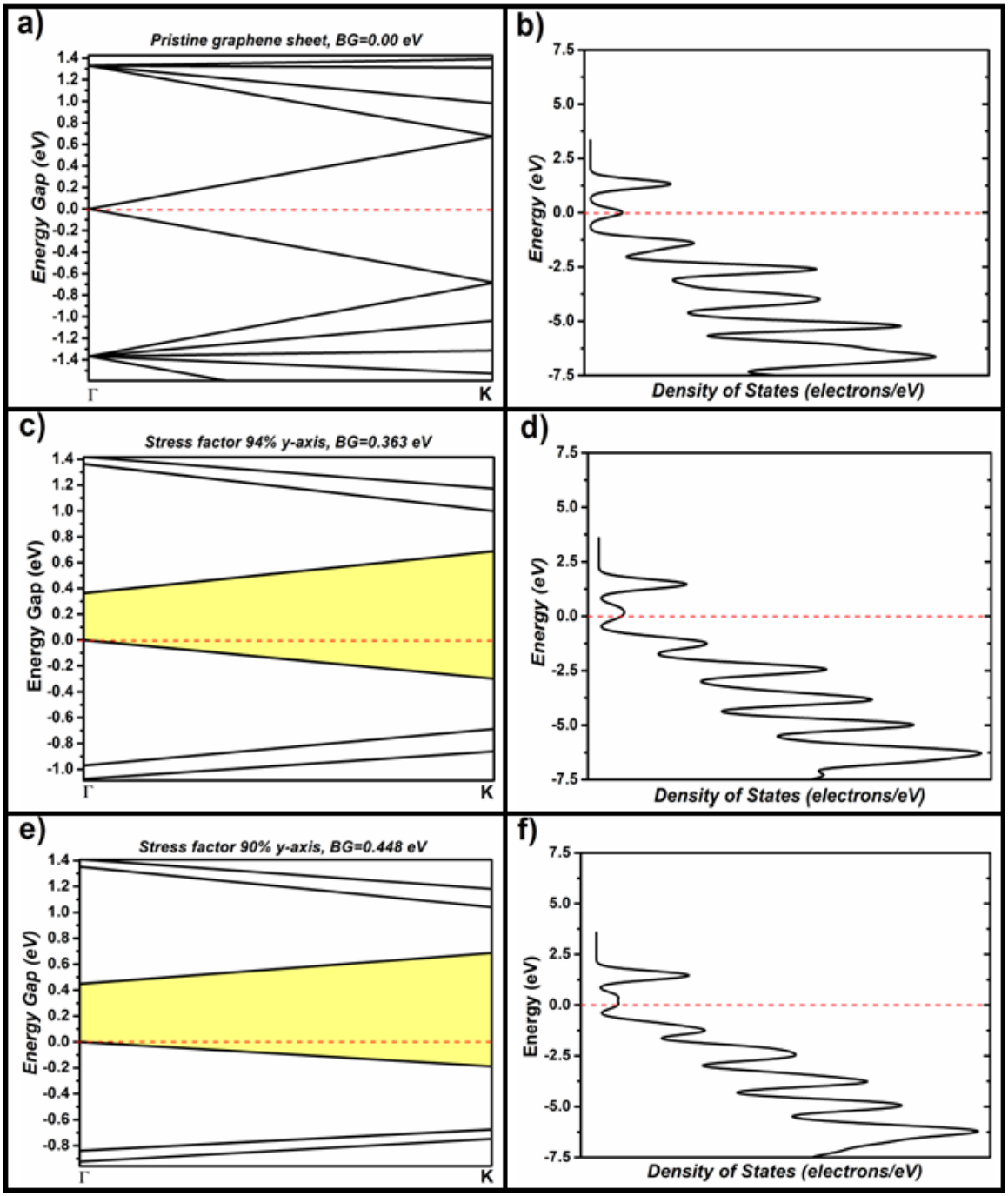

Figure 2: (a, b) Band structure of pristine graphene sheet with its corresponding density of states. (c, d) Band structure of pristine graphene monolayer with its corresponding density of states. (e, f) Band structure of pristine graphene sheet with its corresponding density of states. The red dashed line represents the Fermi energy.

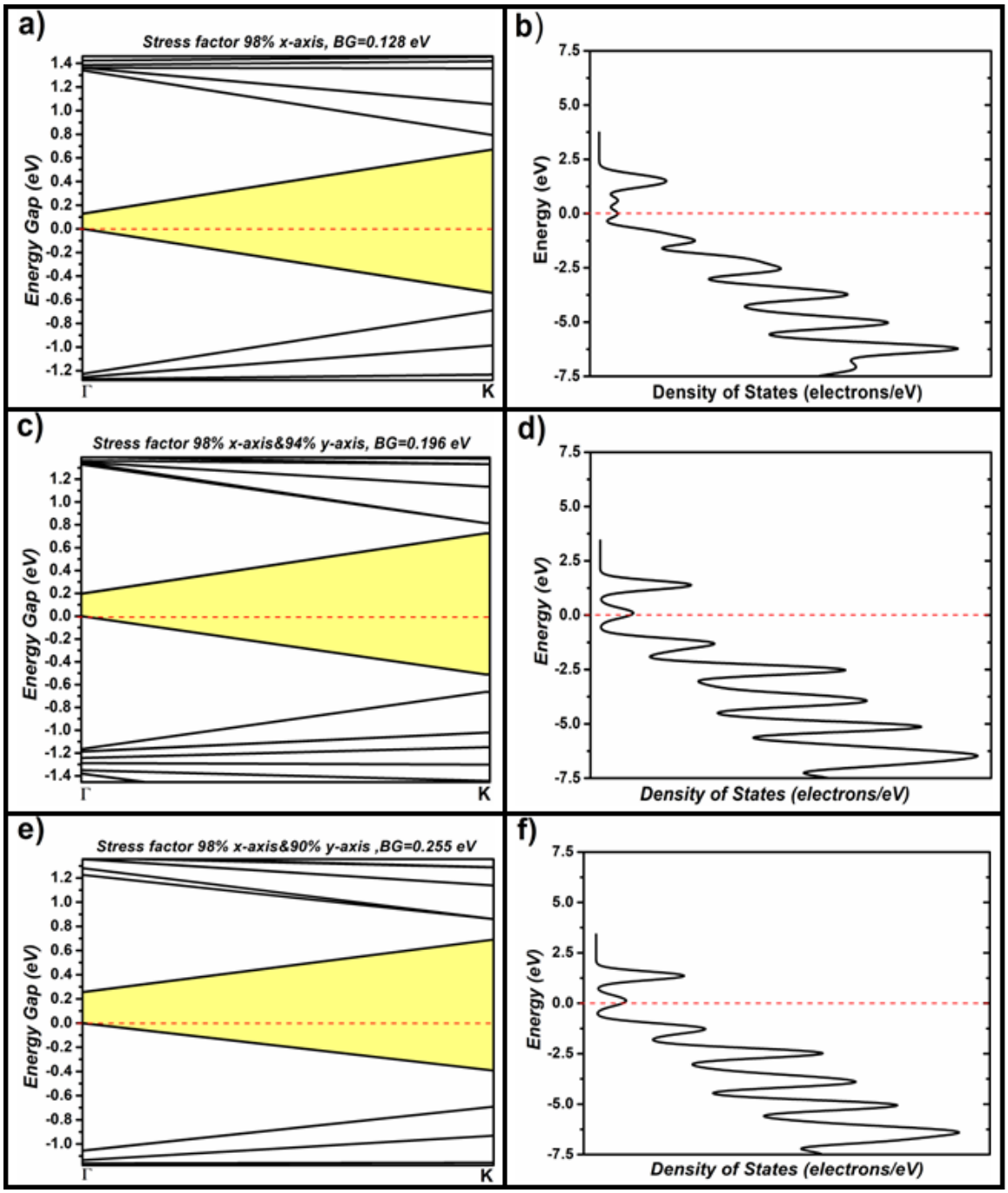

Figure 3: (a, b) Band structure of graphene sheet with stress factor 98% on ***"a"*** and its corresponding density of states. (c, d) Band structure of graphene sheet with stress factor 98% on ***"a"*** and 94% on ***"b"*** and its corresponding density of states. (e, f) Band structure of graphene sheet with stress factor 98% on ***"a"*** and 90% on ***"b"*** and its corresponding density of states. The red dashed line represents the Fermi energy.

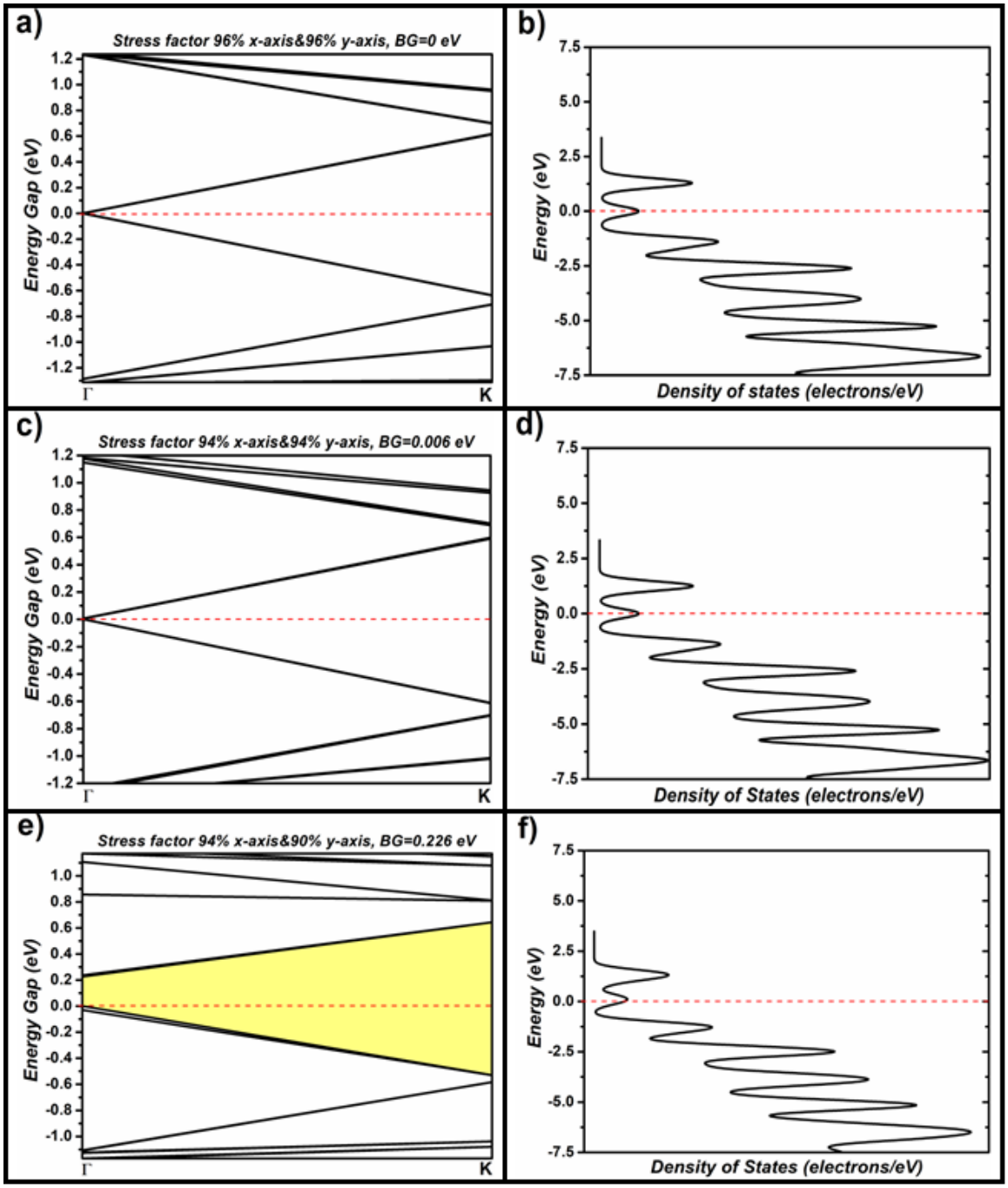

Figure 4: (a, b) Band structure of graphene sheet with stress factor 96% on both ***"a"*** and ***"b"*** and its corresponding density of states. (c, d) Band structure of graphene sheet with stress factor 94% on both ***"a"*** and ***"b"*** and its corresponding density of states. (e, f) Band structure of graphene sheet with stress factor 94% on ***"a"*** and 90% on "b" lattice parameters and its corresponding density of states. The red dashed line represents the Fermi energy.

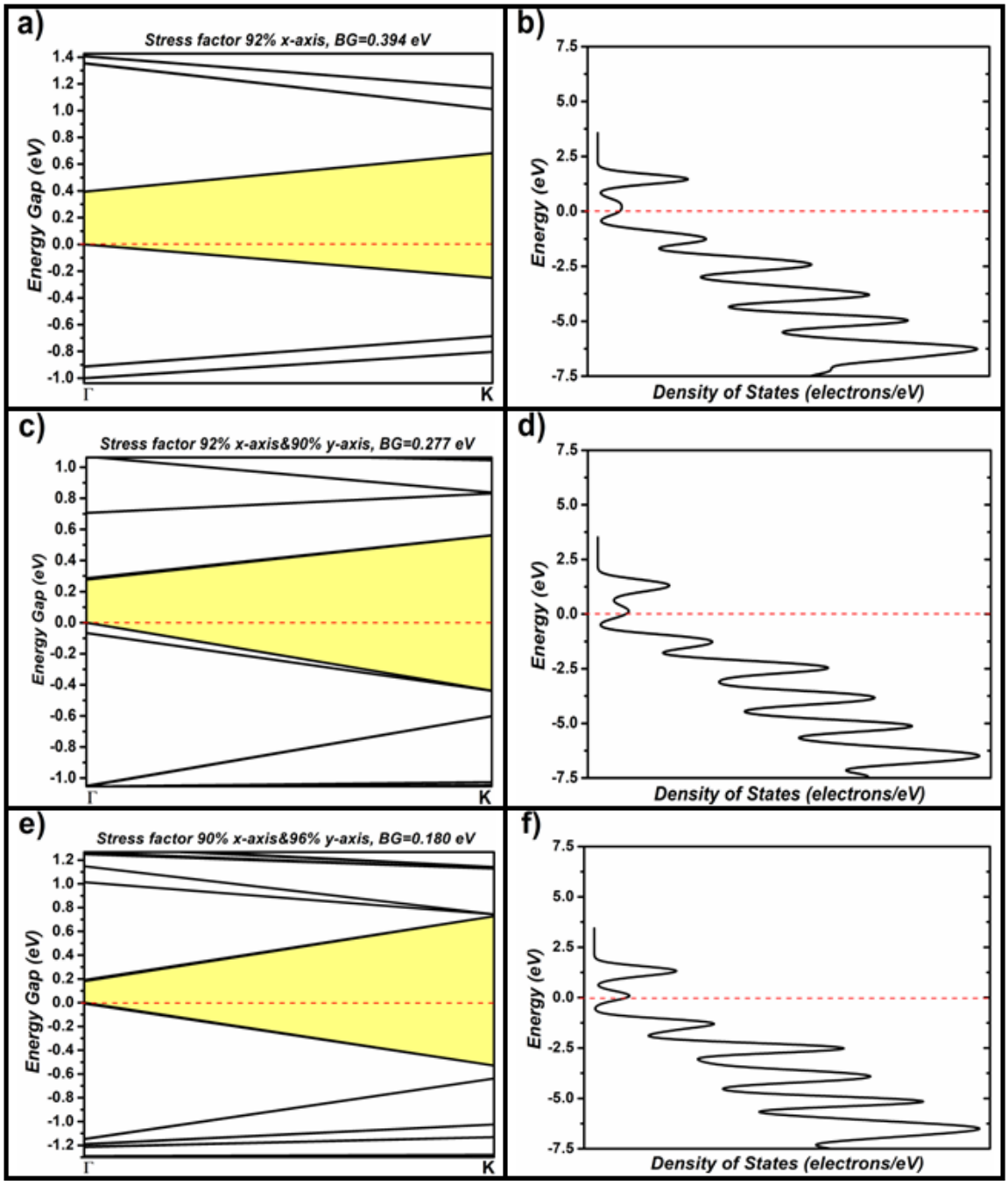

Figure 5: (a, b) Band structure of graphene sheet with stress factor 92% on "a" and its corresponding density of states. (c, d) Band structure of graphene sheet with stress factor 92% on "a" and 90% on "b" and its corresponding Density of States. (e) Band structure of graphene sheet with stress factor 90% on ***"a"*** and 96% on ***"b"*** and its corresponding density of states. The red dashed line represents the Fermi energy.

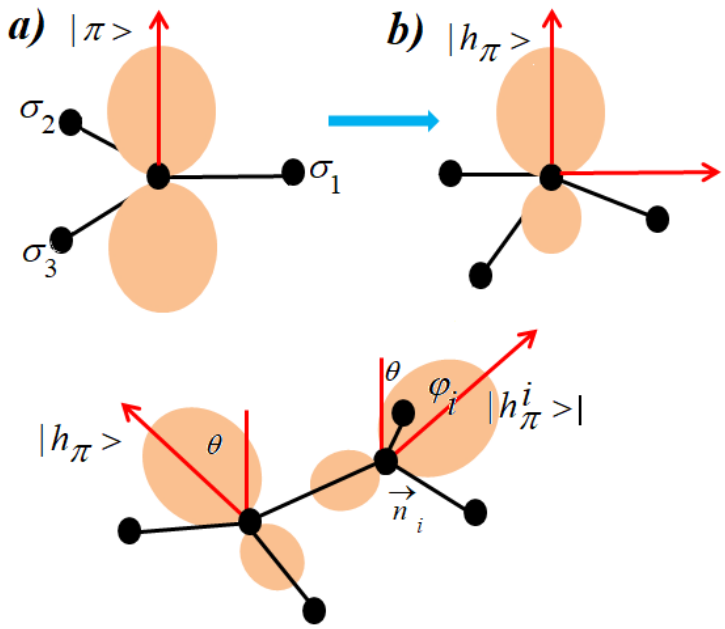

Figure 6: After bending, the pyramid is formed (rippling). (a) Before bending, 3σ bonds are perpendicular to the π orbital, but after bending, the perpendicular structure is changed, and a pyramid structure is produced in the carbon orbitals by introducing a "θ" angle. (b) The orbitals of two C atoms are depicted in a pyramid shape

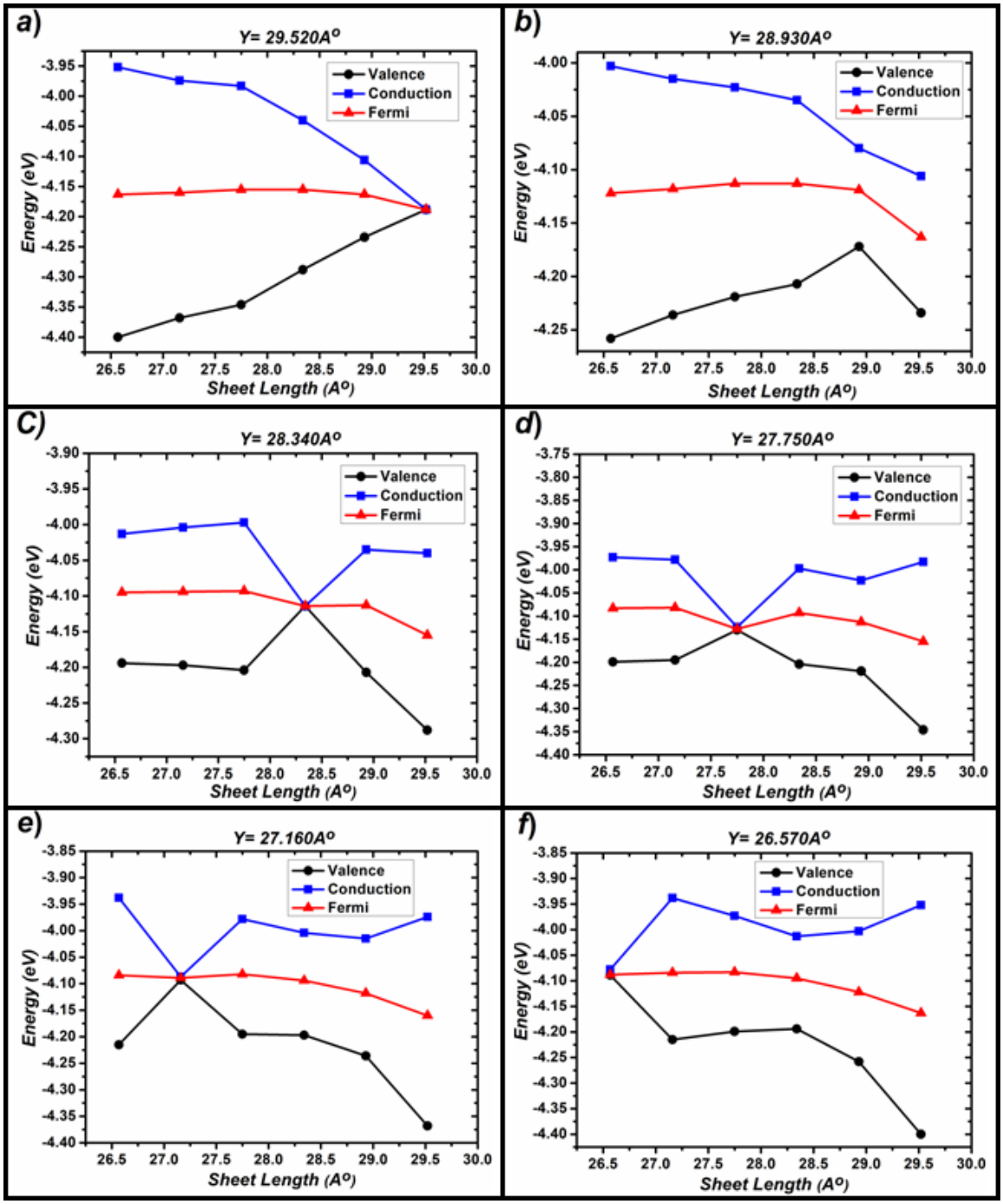

Figure 7: Valence Band, Conduction Band and Fermi Energy vs. graphene monolayer Length.

a (Å) / b (Å)	29.52	28.93	28.34	27.75	27.16	26.57
29.52	0.000 eV	0.128 eV	0.248 eV	0.363 eV	0.394 eV	0.448 eV
28.93	0.128 eV	0.092 eV	0.172 eV	0.196 eV	0.221 eV	0.255 eV
28.34	0.248 eV	0.172 eV	0.000 eV	0.207 eV	0.194 eV	0.180 eV
27.75	0.363 eV	0.196 eV	0.207 eV	0.006 eV	0.216 eV	0.226 eV
27.16	0.394 eV	0.221 eV	0.194 eV	0.216 eV	0.006 eV	0.277 eV
26.57	0.448 eV	0.255 eV	0.180 eV	0.226 eV	0.277 eV	0.011 eV

Table 1: band gap values with respect to the tensile stress factors.